Management 2016, 6(1): 1-10
DOI: 10.5923/j.mm.20160601.01

Static Model Construction for Lower Shuaiba Formation (Lower Dariyan)

Golaleh Zandkarimi*, Ahmad Reza Rabbani

Petroleum Engineering Faculty, Amirkabir University, Tehran, Iran

Abstract Three-dimensional numerical earth models play an increasingly central role in the engineering and petroleum industry. They are routinely used to plan new wells calculate hydrocarbon reserves and when coupled to flow simulator, predict production profile. In the reservoir modeling subject there are different methods for 3D-static modeling of these methods in the present study the geostatistical method is used for 3D-static model of lower shuaiba in the West of Persian gulf. This paper focus on constructing static model for Lower Shuaiba formation is discussed and the 3D static model and property maps showing the oil reserves are presented. Oil in place estimate based on volumetric calculation is finally provided. The static model of Lower Shuaiba formation in the west of Persian Gulf revealed that the major oil deposits lie in the F3 area with some minor deposits in F1, F5 and F8 areas. The oil in place from F3 area amounts to 359.1 MMSTB and from F1, F5 and F8 area are estimated to be around 28.6, 29.9 and 27.9 MMSTB, respectively. Considering the cumulative oil production from Lower Shuaiba being 13.6 MMSTB, 431.9 MMSTB of oil is remaining to be exploited. With a recovery factor of 10% with natural depletion (being on optimistic side) the Lower Shuaiba oil reserve is estimated to be around 31 MMSTB.

Keywords Static model, Oil in place, Volumetric Calculation, Recovery factor

1. Introduction

Generally, models are expressions of our ideas about the encountered problems. Models may be classified as:

Conceptual models (qualitative models)
Physical models (experimental models) for examples:

- Flum-operated simulations of sedimentologic or stratigraphic
- Phenomena at scales ranging from bedforms to basins

Mathematical models (computer models)

- Deterministic models (physical-based or process-based) have one set of input parameters and therefore yield one unique outcome.
- Stochastic models have variable input parameters, commonly derived from probability-density functions (Pdf's) and therefore have multiple outcomes; as a consequence model runs must be repeated many times (realizations) and subsequently averaged.

In 3D-static modeling subject there are different methods. In each of these methods using geological information, mathematical or statistical sciences and different software, properties of the reservoir are modeled. There are some publications in different aspects of the reservoir such as dynamic reservoir simulations (Labourdette et al., 2006; Jachson et al., 2005), fracture intensity (Wong, 2003; Masaferro et al., 2003), 3D stratigraphy, 3D structural model (Mitra and leslie, 2003; Mitra et al., 2006; Hennings et al., 2000).

Geostatistical method is a powerful tool in modeling now. As a historical review the quantification of geology has always been a fascinating topic and of the first pioneering efforts may be noted those Vistelius (1992) and his many followers using Markov chain analysis (Ethier, 1975) to quantify one-dimensional lithological sequences along well. Many successes were encountered with this approach, but it appeared difficult to generalized to the second and third dimensions. Then, in the mid sixties, the giant Hassi Masoud field in Algeria was the object of pioneering application of quantitative reservoir description techniques.

Three realization are different, such a model often consists of hundreds of thousands of grid cells. Current reservoir simulators are not able to handle such large data set and scaling-up heterogeneity models is required before they can be handled by flow simulators. These models will represent the spatial distribution of petrophysical parameters such as porosity and water saturation (Dubrule, 1998).

Generally, geostatistics is study of phenomena that vary in space and/or time. Geostatistics can be regarded as a collection of numerical techniques that deal with the characterization of spatial attributes, employing primarily

* Corresponding author:
a.kasaeipoor@gmail.com (Golaleh Zandkarimi)
Published online at http://journal.sapub.org/ms
Copyright © 2016 Scientific & Academic Publishing. All Rights Reserved

random models in manner similar to the way in which time series analysis characterizes temporal data. In other word, geostatistics offers a way of describing the spatial continuity of natural phenomena and provides adaptations of classical regressions techniques to take advantage of this continuity.

Basic component of geostatistics are:

- Variogram analysis: characterization of spatial correlation
- Stochastic simulation: generation of multiple equiprobable image of the variable also employs semivariogram model. In geostatistics variables are random. A random variable is a variable whose value is a numerical outcome of a random phenomenon (Corstanje et al., 2008). Dataset that use in stochastic are two types. Soft data that measured indirect such are geophysics data and hard data that measure direct in laboratory.

Geostatistics is applied to geological modeling, air pollution, water pollution, mining, biological species. Geostatistical routines are implemented in the major reservoir modeling packages like petrel and Roxar Irap RMS; Used in the generation of grids of facies, permeability, porosity, etc for the reservoir.

Software for representing geology in 3D is routinely used to model subsurface reservoir. The 3D geological modeling or static reservoir modeling technology continue to advance. Software includes some or all of the following capabilities.

- Seismic interpretation, Petrophysical evaluation, Data analysis, Deterministic and geostatistical fault modeling, Deterministic and geostatistical facies/ property models, Uncertainty analysis, Flow based upscaling.

These capabilities allow better integration of seismic data, conceptual geological model, static and dynamic well data into one common earth model.

In the present project the geostatistical method is used for 3D static model of lower shuaiba formation (Lower Dariyan) in the Persian Gulf, in Iran. Structural and petrophysical models for this reservoir were provided using RMS software.

2. Material and Methods

The Lower Shuaiba (Lower Dariyan) formation as a petroleum resrervoir. It is sealed by shales of Kazhdumi formation. 3D geological modeling was made using IRAP-RMS software. All needed data to construct 3D geological model include 3D seismic, well data, (e.g., location, deviation, logs, etc.), well picks (entry point to each horizon) imported to IRAP-RMS data engine. The workflow for geological modeling shall be at least put through following steps:

- Structural modeling
- Fault modeling
- Stratigraphic modeling (construction of layer model)

The definition of the geological model of the reservoir seems to be one of the most important phases in the workflow of a typical reservoir study based on core materials, cuttings, outcrop evidences and logs. To generate this model, we have passed three important phases:

- Structural study: Reviewing the available literature about the regional settings, tectonic evolution of the region, 3D seismic surveys and well information to evaluate the structure top map, its extension and fault pattern.
- Stratigraphic study: Reviewing all the available geology and core reports to infer the sedimetological settings of lower shuaiba reservoir in the Persian Gulf which will help to construct a 3D model of structure.
- Petrophysical properties: Study all the available petrophysical evaluation for the field and data analysis to build the best experimental variogram for stochastic simulation.

Property modeling (stochastic petrophysical modeling) shall be performed using stochastic method. For this purpose simulation method will be used on the basis of actual well data. Quality control of property models will be secured by comparing the statistical results from the model with those of the actual well data.

3. Results and Discussion

Lower Shuaiba (known also as Lower Dariyan) is a tight limestone reservoir. Total cumulative production from Lower Shuaiba is 13 MMSTB, from which 9.4 MMSTB of oil is produced from well F-9-3, a major producer from this reservoir. The reservoir has only a small proportion of the original oil in place.

The static model presented here was constructed based on the structural map from a 3D seismic. Unfortunately, faults model was not available for this study; therefore, faults locations were generated by scanning 2D map of Burgan horizon with faults being shown graphically on the map.

Based on the rock properties, Lower Shuaiba is divided into six layers. This is achieved by cross-correlating all the available well logs within the formation. The available well logs of all the wells were employed in construction of the model presented here.

Cut-off point values applied to Lower Shuaiba formation in calculating net-to-gross (N/G) ratio was 5% for porosity and 50% for water saturation. Because of the relative clean nature of the formation, no clay cut-off was applied. The calculated N/G ratio for this formation was 0.32.

Lower Shuaiba horizon was created by applying average thickness operation in RMS from Burgan A horizon. This approach had to be taken because of lack of horizon of Gadvan. The average thickness between Burgan A and Lower Shuaiba is around 154.28 m. Therefore, by 154.28 m shifting of Burgan A horizon, top of Lower Shuaiba was

created. The created surface was then adjusted to the well points. Similar treatment was applied to create the rest of the horizons. The final 3D structural map created for Lower Shuaiba formation is given in Figure 1.

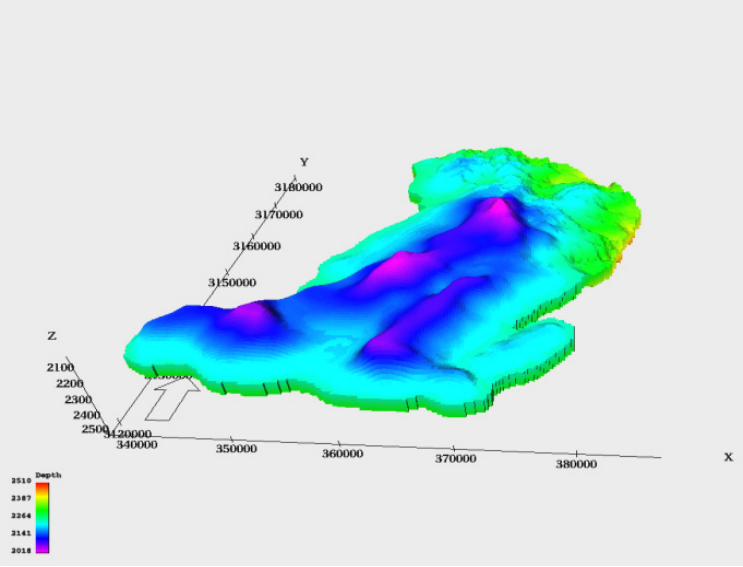

Figure 1. 3D structural map for Lower Shuaiba

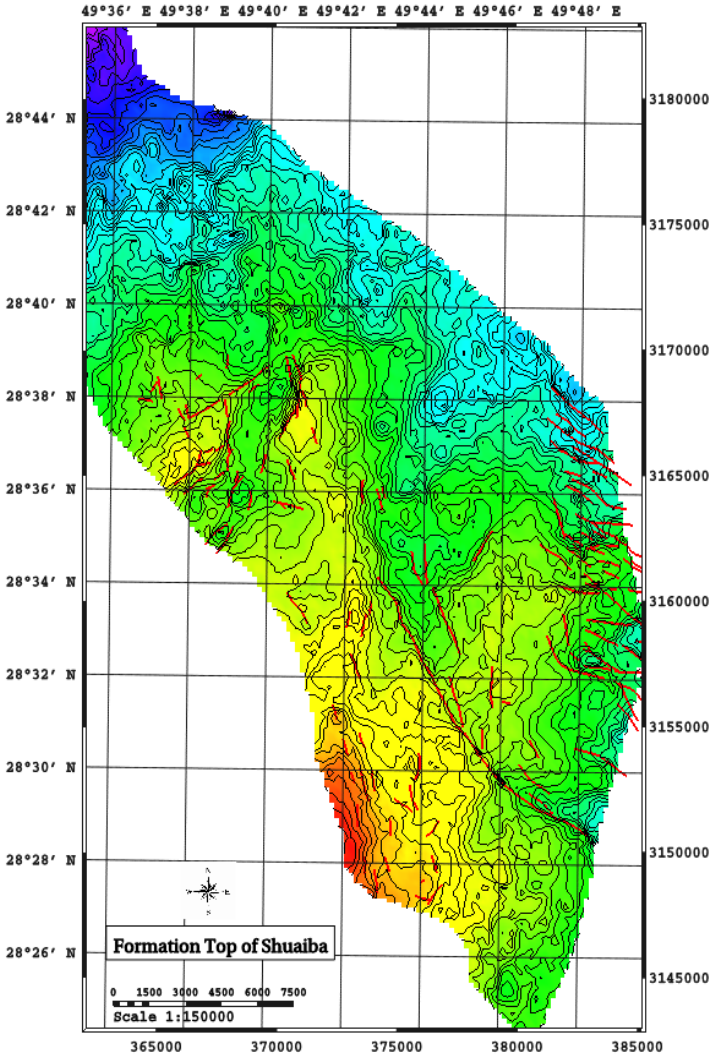

Figure 2. Faults map for Shuaiba formation from 3D seismic interpretation

3.1. Creating Wells and Importing Well Survey Data

All the wells drilled into the Lower Shuaiba formation were imported into the model. Those wells from this comprehensive list that were drilled in Lower Shuaiba formation were used for construction of this model. Well logs from those wells that penetrated the full thickness of Lower Shuaiba formation were re-interpreted and imported into the model.

3.2. Fault Mapping

As shown in Figure 2, generated from 3D seismic interpretation, Lower Shuaiba formation contains significant number of faults. However, because of lack of faults model, fault mapping was constructed only for the five major faults. Fault location was detected from 2D depth map with faults. The map was digitized and faults were imported into the formation structure. No fault displacement could be generated from the map and the faults were assumed to be vertically penetrating the whole formation thickness. Figure 2 which was generated from one specific level does not reveal all the five major faults. However, inspecting similar maps for various levels confirms presence of the five major faults. Figure 3 presents the five major faults for Lower Shuaiba formation and Figure 4 illustrates the segmentation of Lower Shuaiba resulted from the presence of these major faults. Figure 5 presents 3D structural map of lower Shuaiba with the location of five major faults.

Figure 3. Major faults for Lower Shuaiba formation

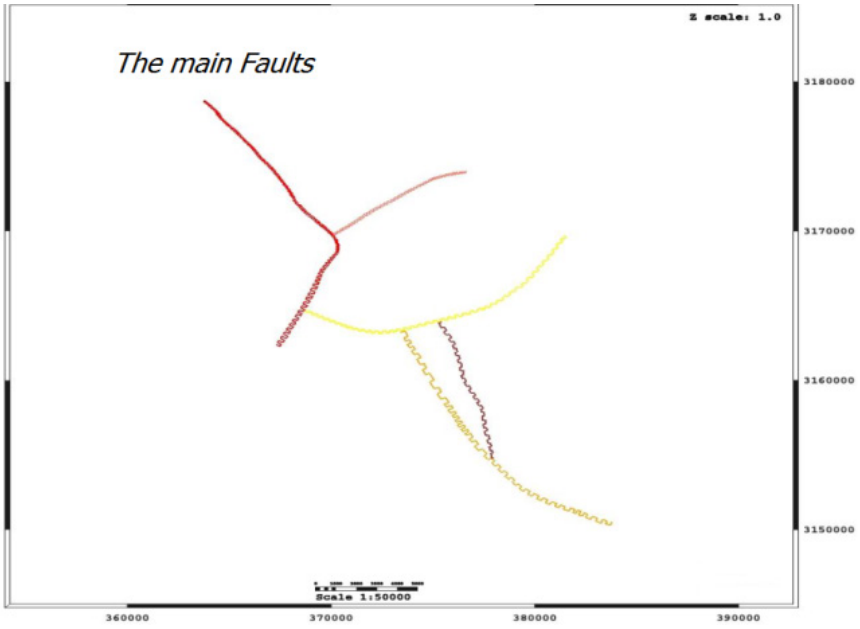

Figure 4. Segmentation of Lower Shuaiba formation

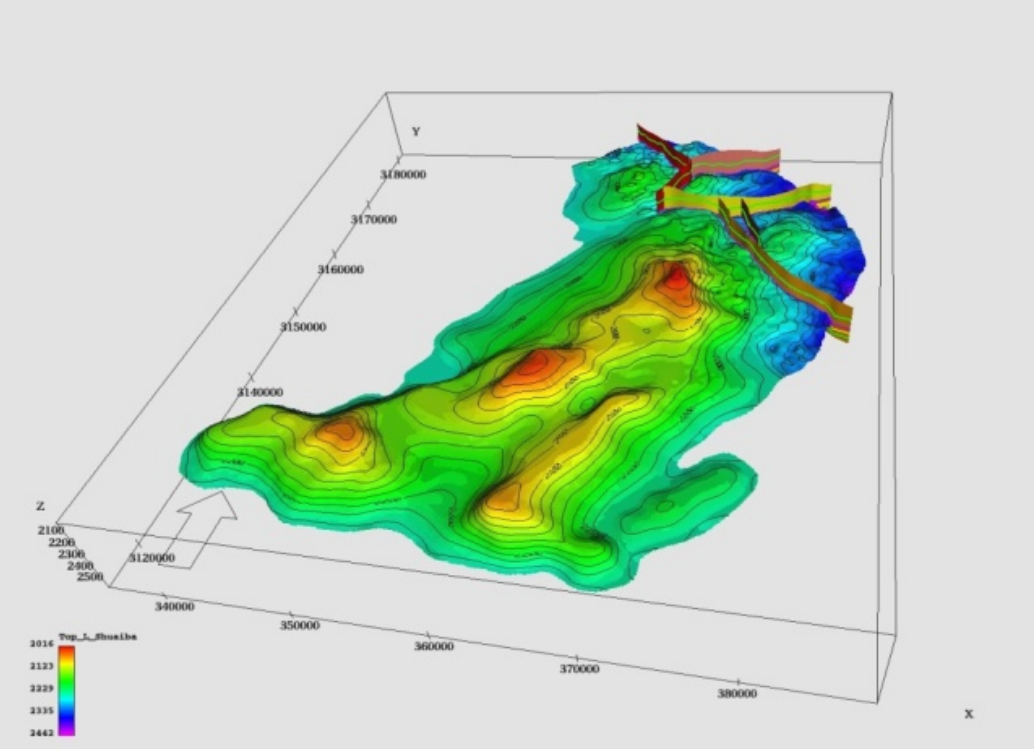

Figure 5. 3D structural map of Lower Shuaiba with the five major faults

3.3. Property Mapping

Reservoir properties such as porosity and water saturation were imported into the structural map by using the interpreted logs of all the existing wells. Water-oil-contact was then located on the map. Lower Shuaiba, being an undersaturated reservoir, did not produce any gas-oil-contact. Water-oil contact does not seem to be the same for various areas. Even for a given production zone a variable water-oil contact is depicted. To handle the variable water-oil contact in the model, it was decided to select a fixed water-oil contact for each region and adjust it by applying appropriate capillary pressure curve for transition zone saturation calculation. That is why various capillary pressure curves for various regions are defined based on water saturation distribution versus depth generated for each region from corresponding available well logs.

By plotting water saturation versus depth for various wells, it was noticed that wells are clustered into three distinct regions. The upper, lower and middle regions are elongated from northwest to southeast. The upper region wells are those wells drilled on the crest and the middle and lower regions are those wells drilled in the flank of the structure. that formation could be divided into six distinct layers with distinct reservoir properties. Therefore, the capillary pressure curves for the three regions are needed to properly characterize transition zones in various rock types. However, by further investigation it was felt that the wells in the two flank regions could be approximated by single rock type from capillary pressure point of view. Therefore, the wells were divided into two regions of crest and flank as shown in Figure 6 by color coding location of the wells. Layer 6 which is a poor quality rock can also be represented by a single capillary pressure curve. The application of these capillary pressure curves for determining water saturation distribution in the transition zone is implemented during setting up the corresponding dynamic model. Here, only one single average capillary pressure is being used for assigning water saturation in transition zones. Therefore, the original oil in place estimated here should be viewed as approximate and its final refinement will be achieved during dynamic modeling.

Water saturation distribution for each individual production area is given in Figures 7 to 12 and for the total area is presented in Figure 13. Water saturation distribution of F3 area within the transition zone was determined based on well logs interpretation as well as by applying capillary pressure curve which are presented in Figures 8 and 9, respectively. The capillary pressure curve used in this calculation was generated from well logs water saturation versus depth. Water saturation versus depth generated from well logs is presented in Figure 14 and the corresponding capillary pressure is given in Figure15. Similar treatment was applied for F1 and F5 areas. However, one single capillary pressure curve was applied for both areas. The water saturation distribution versus depth generated from well logs and the corresponding capillary pressure curve for this case are given in Figures 16 and 17, respectively. No capillary pressure was applied for F8 area. Its water saturation distribution was determined based on the interpreted well log data and the water-oil contact was assumed to be the same as its spill point.

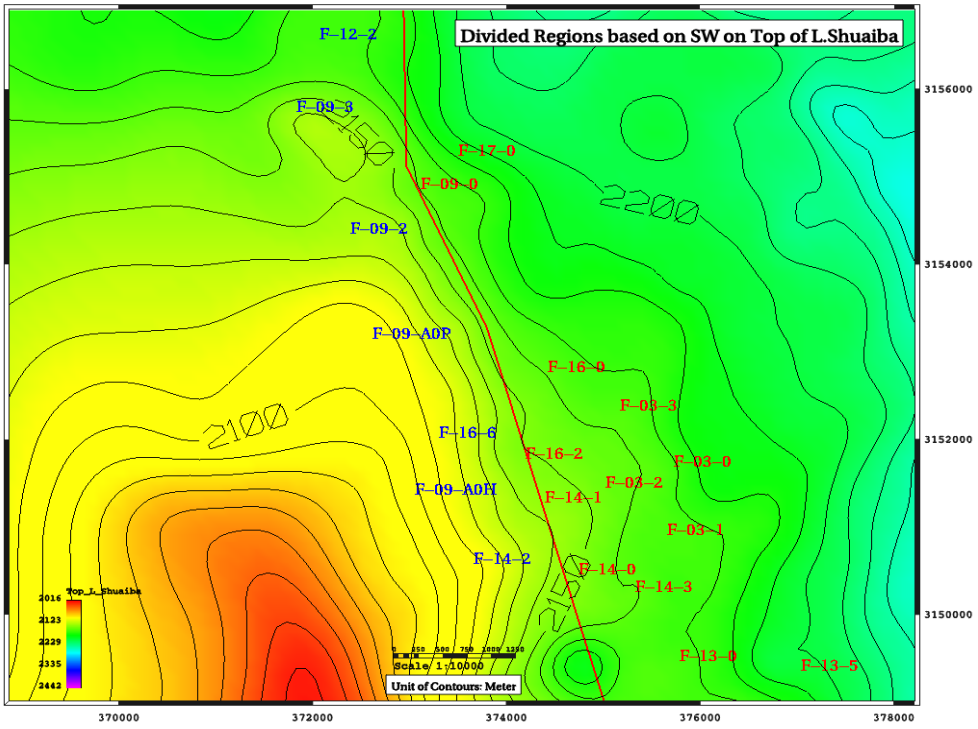

Figure 6. Flank and crest region of Lower Shuaiba detected by well logs re-interpretation

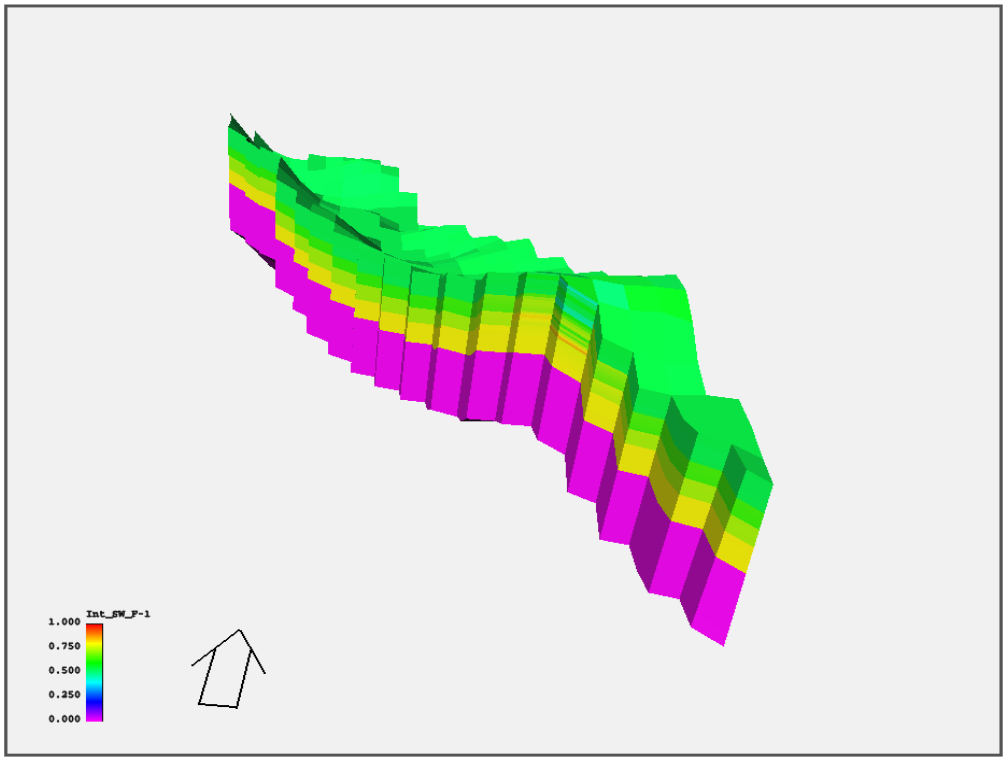

Figure 7. 3D view of Lower Shuaiba water saturation distribution in F1 area

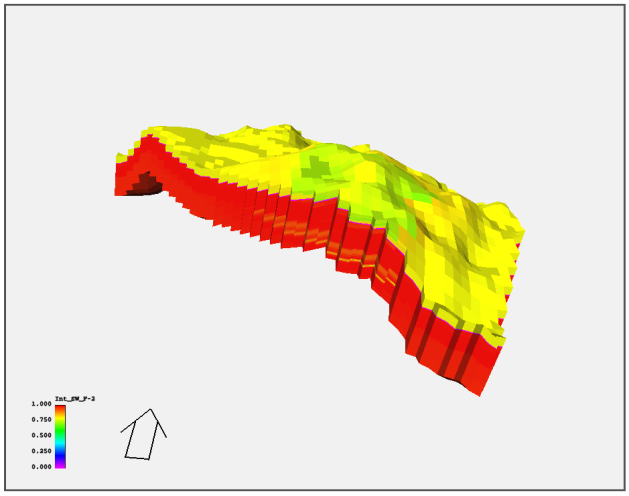

Figure 8. 3D view of Lower Shuaiba water saturation distribution in F2 area

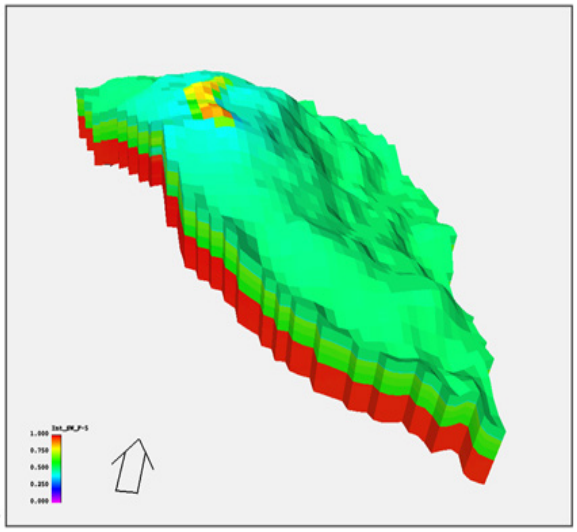

Figure 11. 3D view of Lower Shuaiba water saturation distribution in F5 area

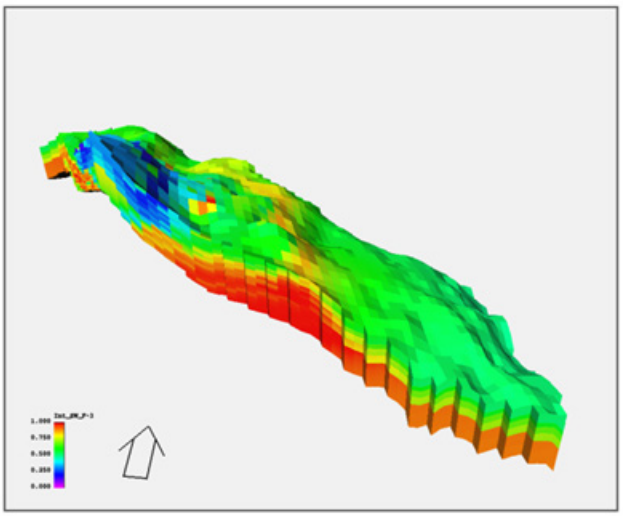

Figure 9. 3D view of Lower Shuaiba water saturation distribution in F3 area based on log interpretation

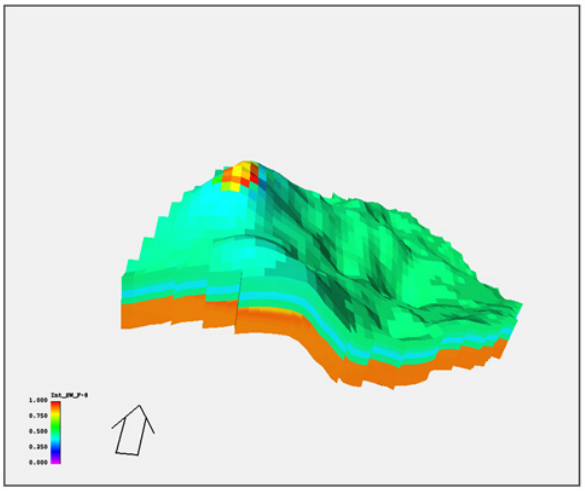

Figure 12. 3D view of Lower Shuaiba water saturation distribution in F8 area

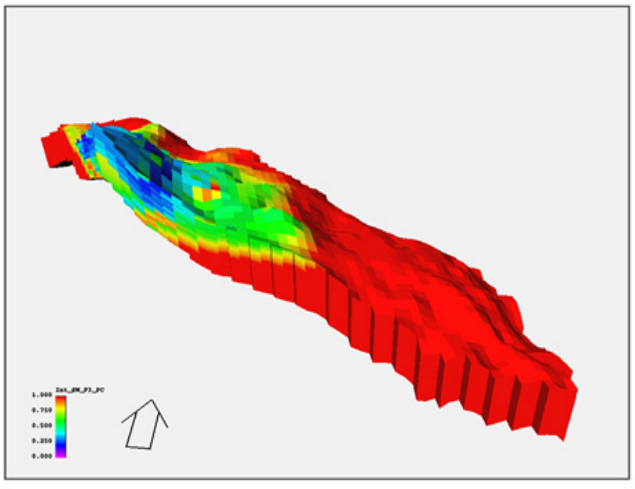

Figure 10. 3D view of Lower Shuaiba water saturation distribution in F3 area based on capillary pressure application for transition zone

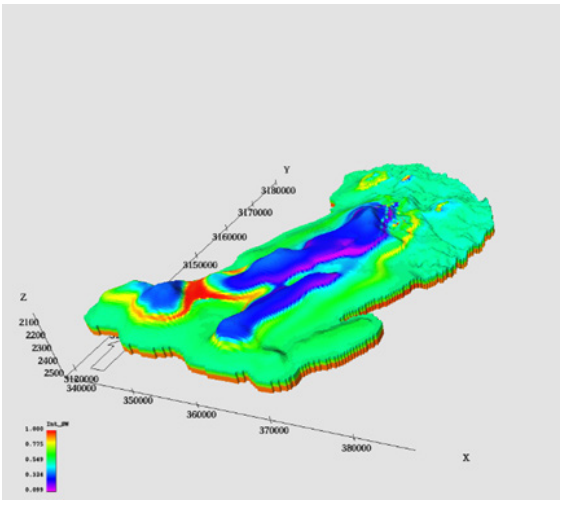

Figure 13. 3D view of Lower Shuaiba water saturation distribution for all areas

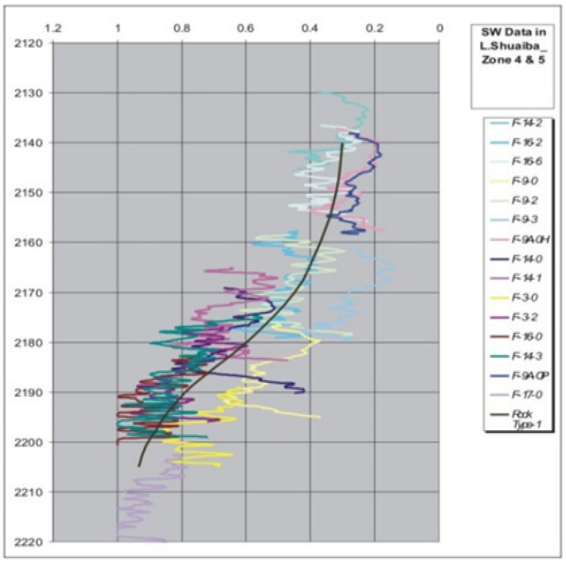

Figure 14. Depth versus water saturation derived from well logs

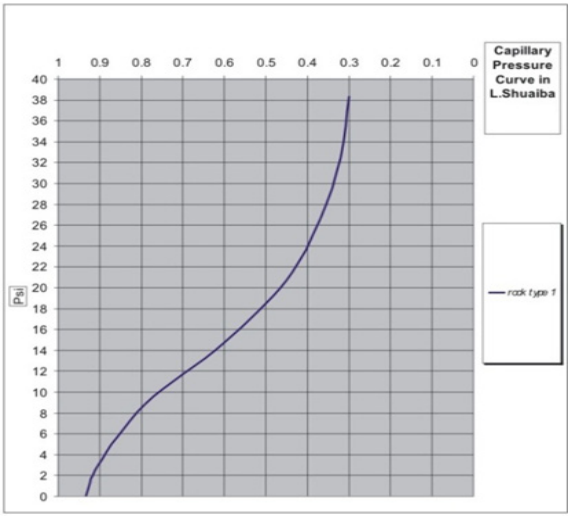

Figure 15. Capillary pressure curve used for water saturation distribution calculation in transition zone for F3 area

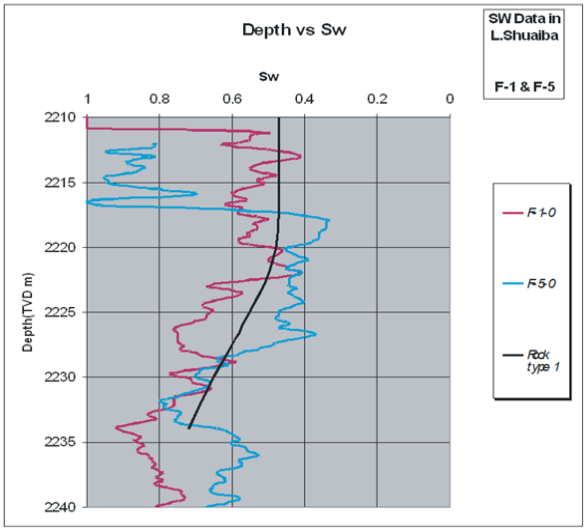

Figure 16. Depth versus water saturation derived from well logs for F1 and F5 areas

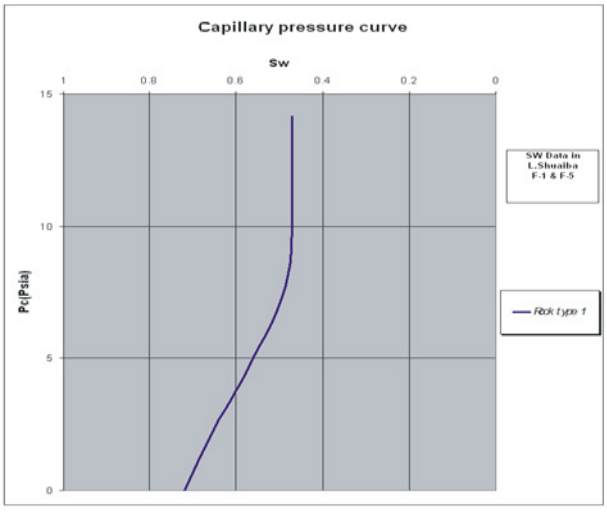

Figure 17. Capillary pressure curve used for water saturation distribution calculation in transition zone

The oil bearing regions are demonstrated by green color in Figures 18 to 25 for F1, F3, F5, and F8 regions, respectively. The major portion of the oil deposits is evidently detected in F3 area and some minor amount in F8 area. F2 area is a water-bearing zone which has not been shown here.

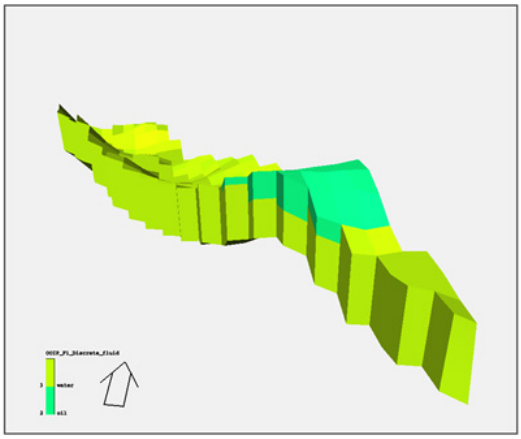

Figure 18. 3D view of Lower Shuaiba formation showing the oil zone in F1 area

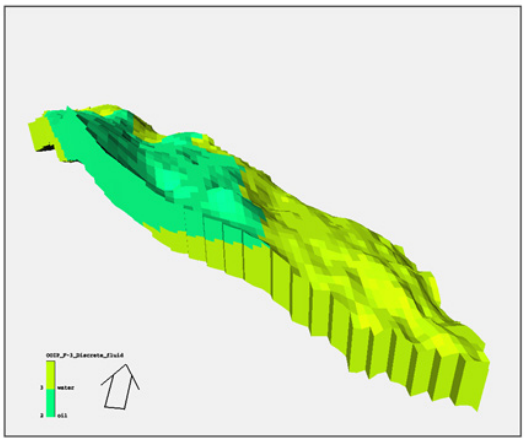

Figure 19. 3D view of Lower Shuaiba formation showing the oil zone in F3 area

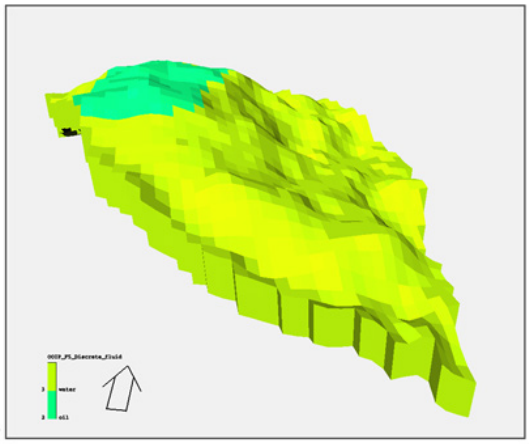

Figure 20. 3D view of Lower Shuaiba formation showing the oil zone in F5 area

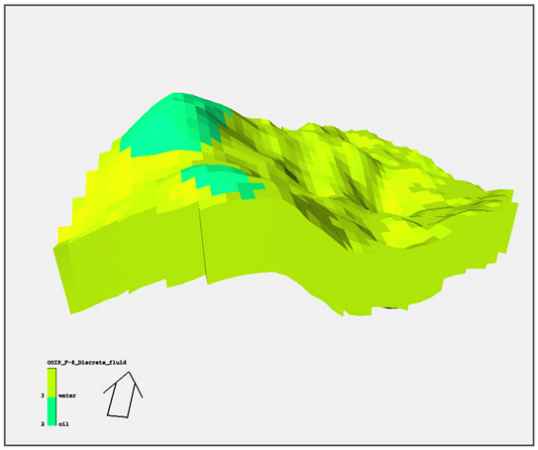

Figure 21. 3D view of Lower Shuaiba formation showing the oil zone in F8 area

3D porosity map is presented in Figure 22 for Lower Shuaiba formation. Figure 23 presents a 3D cross-sectional view of the porosity distribution with water-oil contact being illustrated. The oil-bearing regions become evident from this figure being located above the water-oil contact line.

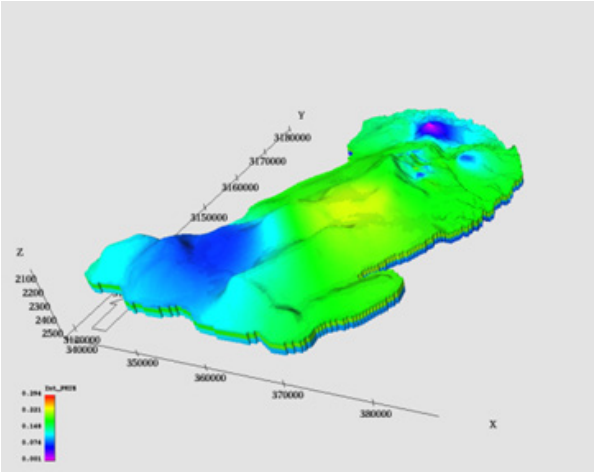

Figure 22. 3D porosity map of Lower Shuaiba formation

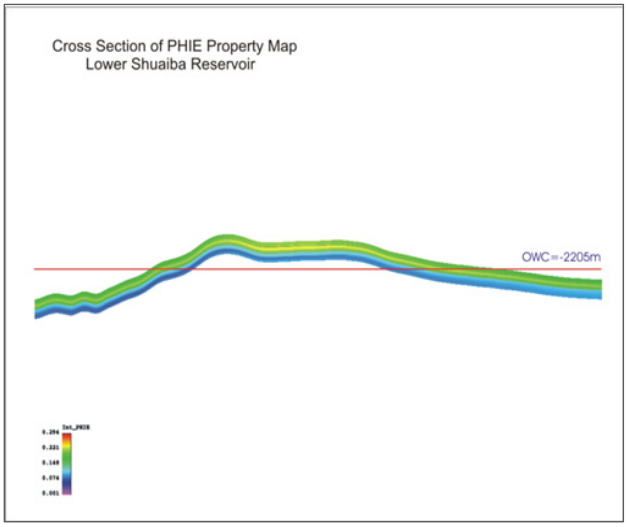

Figure 23. 3D cross-sectional view of porosity map with water-oil contact for Lower Shuaiba formation

3.4. Oil in Place

Oil-In-Place (OIP) and solution Gas-In-Place (GIP) estimation based on volumetric calculation for the four detected oil-bearing regions were performed. Results are presented in Table 1. Values of 1.37 Res. bbl/STB and 590 SCF/STB were used for oil formation volume factor and solution gas/oil ratio in this calculation, respectively. For the sake of comparison and to reveal the future oil production potential, cumulative oil production from the corresponding area is also included in Table 1. It is evident from Table 1 that most of the oil deposits are stored in F3 area and much smaller portion in F1, F5 and F8 area. F2 area in completely watered out and is not included in this table. The oil in place for F3 area amounts to 359.1 MMSTB while that in F1, F5, and F8 area is less than 30 MMSTB. That is, the total amount of original oil in place for the Lower Shuaiba formation is estimated to be around 445.5 MMSTB. It should be realized that most of the oil in F1 and F5 areas is in the transition zones. Considering a recovery factor of 10% with natural depletion (being on optimistic side) a total reserve of 31 MMSTB of oil is expected from this formation to be included in MDP II.

Table 1. Oil-In-Place (OIP) and Gas-In-Place (GIP) for Lower Shuaiba formation

Zone	OIP MMSTB	Reserve MMSTB	GIP, BSCF		Cum. Prod. MMSTB
			Free Gas	Dis. Gas	
F1	28.6	2.86	0.0	16.9	0.0
F3	359.1	22.32	0.0	211.9	13.59
F5	29.9	2.99	0.0	17.6	0.0
F8	27.9	2.79	0.0	16.5	0.0
Total	445.5	30.96	0.0	262.9	13.59

4. Conclusions

Based on rock properties of lower shuaiba, this formation is divided into six layers. Layer 3 is the main producer layer with average thickness of 7 m and an average porosity 17%. Layer 4 is the second producer layer with average thickness of 10.5 and an average porosity 18%.

Total cumulative production from Lower Shuaiba was 13 MMSTB, from which 9.4 MMSTB of oil was produced from well F-9-3, a major producer from this reservoir. The reservoir has only produced a small proportion of the original oil in place.

According to water saturation versus depth curves for various wells, these are classified three regions. The upper, middle and lower regions are elongated from northwest to southeast. The upper region wells are those wells drilled on the crest and the middle and lower regions are those wells drilled in the flank of the structure.

REFERENCES

[1] Corstanje, R., S. Grunwald and R.M. Lark, 2008. Inferences from fluctuation in the local variogram about the assumption of stationary in the variance. Geoderma, 143; 123-132.

[2] Dubrule, O., 1998. Geostatistics in petroleum geology. AAPG continuing education course note series No. 38, Tulsa, Oklahoma, USA.

[3] Ethier, V.G., 1975. Application of Markov analysis to the Banff formation (Mississippian), Alberta. Math. Geo., 7: 47-61.

[4] Hennings, P.H, J.E. Oslon and L.B. Thompson, 2000. Combining outcrop data and three- dimensional structural models to characterize fracture reservoir. An example from Wyoming. AAPG Bul., 84: 830-849.

[5] Jackson, M.D., S. Yoshida, A.H. Muggeridge and H.D. Jahnson, 2005. Three-dimensional reservoir characterization and flow simulation of heterolithic tidal sandstones. AAPG Bul., 89: 507-528.

[6] Masaferro, J.L., M. Bulnes, J.Poblet and N. Casson, 2003. Kinematic evolution and fracture prediction of the valle morado structure inferred from 3D seismic data, salta province, northwest Argentina. AAPG Bull., 87: 1083-1104.

[7] Mitra, S. and W. Leslie, 2003. Three dimensional structural model of the Rhourde el Baguel field, Algeria. AAPG Bull., 87: 231-250.

[8] Mitra, S., J.A.D. Gonzalez, J.G. Hernandez, S.H Garcia and S. Banerjee, 2006. Structural geometry and evolution of the Ku, Zaap and Maloob structures, Campeche Bay, Mexico. AAPG Bull., 90: 1565-1584.

[9] Wong, P.M., 2003. A novel technique for modeling fracture intensity: A case study from the Pinedale anticline Wyoming. AAPG Bull., 87: 1717-1727.